Wind farm revenues in Western Europe in present and future climate

Alonzo B., Tankov P., Creti A., Concettini S., Drobinski P.

April 7, 2020

Abstract

We quantify the revenues and net present value of wind farms in France, Germany and Denmark, as well as their variability, under present and future climate. The present climate study is based on ERA20C reanalysis covering the 20th century to generate climate scenarios, and quantifies the sensitivity of wind farm revenues and value to the natural variability of climate. The study using future climate data is based on CORDEX climate projections and integragted assessment model scenarios, and quantifies the effect of climate change on the value and revenues of wind farms.

Key words: wind energy, climate variability, climate change

1 Introduction

To limit greenhouse gases emissions from power generation, the use of renewable intermittent energy sources, such as wind and sun, has been encouraged in many European countries. Renewable energy generation together with the electrification of carbon-intensive sectors such as transport and heating, are the pillars of energy transition. In this context, wind energy plays a particularly important role because of high wind potential in Europe, rapidly decreasing costs of technology, regulated support mechanisms and good acceptance by the public. However, to achieve energy transition objectives, a large amount of investment in this sector is still needed. According to the latest available data, in 2018 the European wind sector has attracted investments for 65 billion euros and this figure is expected to increase in the short term due to favourable economic conditions [WindEurope, 2019].

While the socio-economic context seems favourable for investment in wind energy, the natural variability of the wind resource makes investment risks difficult to manage; moreover, climate change is likely to impact not only future wind energy production but also electricity prices. A more precise understanding of the risks at stake should enable the financial industry to develop suitable funding instruments and to become a key actor in fighting the climate disruption and its adverse effects.

The objective of this paper is therefore to quantify the uncertainties of future revenues and the net present value of virtual wind farms[1] in three Western European countries, namely France, Germany and Denmark. The first source of uncertainty is related to the variability of the capacity factors of wind farms in the long term. Many studies assess the variability of the wind speed and of energy production at long timescales (see for instance [Pryor et al., 2006, Boccard, 2009, Grams et al., 2017]). These papers relate long-term wind variability to large scale weather patters such as the North Atlantic Oscillation (NAO). Another strand of literature analyses the impact of climate change on wind speed and energy production [Pryor et al., 2005, Pryor and Barthelmie, 2010, Tobin et al., 2015, Tobin et al., 2016]: these works highlight a slight decrease in wind energy production and conclude that the long term natural variability of wind resource, driven by large-scale weather patterns, dominates the climate change signal. These results may be summarised by saying that the wind resource is not expected to undergo significant changes and its long-term variability seems to remain largely dominated by the well known, but still unpredictable, large-scale weather patterns.

The second source of uncertainty is related to the price at which the generated energy is sold, and is thus mostly driven by the wholesale electricity prices.[2] Spot electricity prices are function of electricity demand, which is strongly correlated with temperature. With the advent of climate change, electricity demand is expected to decrease in many countries due to rising winter temperatures [Wenz et al., 2017, Damm et al., 2017]. A North/South polarization of the demand can also be expected [Wenz et al., 2017]. These studies only account for temperature changes and do not consider the potential impact of large-scale electrification. Electricity prices also depend on renewable energy penetration: this source of energy has low marginal cost and tends to decrease wholesale equilibrium prices by displacing higher cost technologies, the so-called "merit-order effect" (see for instance [Cludius et al., 2014, Clò et al., 2015]). To the best of our knowledge, the combined effect of temperature and wind speed variability on wholesale price trend and variability has not been thoroughly analysed.

The revenues of wind farms are of course strongly affected by the support mechanisms in place [Gatzert and Vogl, 2016]. This paper adresses the case of feed-in-tariff (FiT) and feed-in-premium (FiP), because they have been and are still widely used to support wind energy and other renewables. Other sources of uncertainty, such as public acceptance of wind farms ([Hitzeroth and Megerle, 2013]), have been already discussed in the literature and go beyond the scope of this work. For a complete overview of wind farm investment risk sources, the reader may refer to [Gatzert and Kosub, 2016].

Our study is organized in two parts. In the first part, we model the revenues and quantify the net present value of virtual wind farms based on historical wind and temperature data spanning the 20th century. Historical data allow to disentangle the different sources of variability and to quantify the variations in the revenues and expenditure of virtual wind farms at current natural variability, market design and network structure,

---

[1]Virtual refers to the fact that we are not estimating the value of a specific existing wind farm, but the value of a generic wind farm in a given location and with given characteristics.

[2]Other revenues may be generated by Green Certificates, CO2 allowances, etc.

under different support schemes. In the second part, we generate future price scenarios using electricity demand and renewable penetration projections from integrated assessment models. These are combined with wind speed and temperature projections from the regional climate model intercomparison project (CORDEX), corresponding to several Representative Concentration Pathways (RCP). This enables us to model future local wind energy production and prices in a changing climate. This approach allows to assess and quantify the three sources of uncertainty identified in the [I4CE, 2019] report, namely : socio-economic uncertainties corresponding to the choices made by the society (e.g the extent climate change mitigation vs. adaptation), scientific uncertainties (corresponding to model simulations spread and associated with modeling errors), and natural/climate uncertainties (related to the natural variability of the earth system, including climate change).

The rest of the paper is structured as follows. The next section describes the meteorological data we employ and the models used to transform it into realistic scenarios of electricity prices and wind energy production. In this section, we also give a precise definition of wind farm revenues and wind farm value indicators used in the study. In Section 3, we analyze the variability of wind farm revenues and net present value based on historical data. In Section 4, future price projections are used to project future wind farm revenues until 2050 and estimate their net present value under future climate. The last section gives the main conclusion of the paper.

2 Data & Methods

2.1 Description of datasets

This study is based on historical energy consumption, energy production and electricity price data at the national level and on meteorological data from reanalysis as well as from regional climate models (RCM) at the local scale (model gridpoints).

From the European Network of Transmission System Operators for Electricity (ENTSOE) website, we retrieve the hourly demand (D_n), production (W_n) and day-ahead price (P_n) for France, Germany and Denmark between January 1, 2015 and December 31, 2018. From the RTE (Réseau de Transport d'Électricité) website, we retrieve the observed regional monthly wind capacitify factor in the French regions between January 2015 and December 2017.

As a proxy for past climate, from ERA-5 reanalysis ([Hersbach and Dee, 2016]) and ERA-20C reanalysis ([Poli et al., 2016]), we retrieve surface temperature (T_{2m}), and surface wind speed (F_{10m}) over the domain covering France, Germany and Denmark (Figure 1). The ERA-20C reanalysis spans the period from January 1, 1900 to December 31, 2010, at the 6-hourly time resolution and the spatial resolution is 1.125°. The ERA-5 reanalysis spans the period from January 1, 1979 to December 31, 2018, at the hourly time resolution and the spatial resolution is 0.25°. The ERA-5 data is used to link the observations with the ERA-20C data which do not overlap with observed data. Table 1 summarizes the data retrieved from reanalysis datasets as well as from the ENTSOE

website.

Sources	Variable	Name	Period	Time resolution
ENTSOE	Electricity Demand	D_n	Jan 1, 2015 to Dec 31, 2018	hourly
	Wind production	W_n	Jan 1, 2015 to Dec 31, 2018	hourly
	Day-ahead prices	P_n	Jan 1, 2015 to Dec 31, 2018	hourly
ERA-5	Surface Temperature	T_{2m}	Jan 1, 1979 to Dec 31, 2018	hourly
	Surface wind speed	F_{10m}	Jan 1, 1979 to Dec 31, 2018	hourly
ERA-20C	Surface Temperature	T_{2m}	Jan 1, 1900 to Dec 31, 2010	6-hourly
	Surface wind speed	F_{10m}	Jan 1, 1900 to Dec 31, 2010	6-hourly
CORDEX (see table 2)	Surface Temperature	T_{2m}	Jan 1, 1971 to Dec 31, 2005 and Jan 1, 2006 to Dec 31, 2100	daily
	Surface wind speed	F_{10m}	Jan 1, 1971 to Dec 31, 2005 and Jan 1, 2006 to Dec 31, 2100	daily

Table 1: Summary of the data used in the study

As future climate projections, we use simulations from the Coordinated Regional Downscaling Experiment (CORDEX) program ([Giorgi et al., 2008]) which aims at developing an improved framework for generating regional-scale climate projections. We retrieve daily surface temperature and daily surface wind speed from historical, RCP-4.5 and RCP-8.5 simulations of several Regional Climate Models (RCMs) listed in the table 2 over the European domain (EUR44) with spatial resolution of 0.44°. The historical simulations span from Jan 1, 1971 until Dec 31n 2005, and the RCP-4.5 and RCP-8.5 simulations span the period from Jan 1, 2006 until Dec 31, 2100. In this paper, we limit the period of study to Dec 31, 2050.

Institution	Model used
IPSL-INERIS	IPSL-CM5A-MR
DMI	ICHEC-EC-EARTH
CLM-Com	MPI-M-MPI-ESM-LR
MPI-CSC	MPI-M-MPI-ESM-LR
SMHI	NOAA-GFDL-ESM2M

Table 2: List of the CORDEX model simulations used in the study

Onshore (Figure 1-a, b, c) and offshore (Figure 1-d, e, f) masks are drawn for each country to make the difference between onshore wind farms which have a lower capacity factor and lower costs, and offshore wind farms.

2.2 Model schemes

Price scenarios Figure 2 shows the process for modelling day-ahead prices in each of the three countries considered. The scheme is decomposed into three steps. The aim of the first step is to correct the bias in the long time series of wind speed and surface
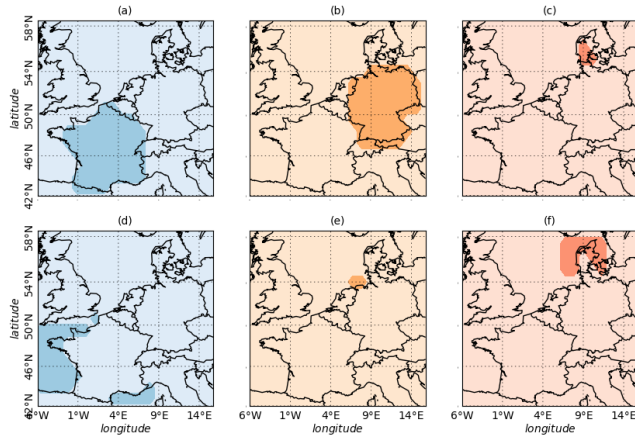
Figure 1: Domains and onshore and offshore masks in ERA20C data

temperature (ERA-20C and Cordex simulations) using the shorter time series of ERA-5, considered more reliable. To this end, we consider the ERA-5 data as observations and apply a quantile/quantile correction between 6-hourly surface temperature and daily wind speed from ERA-5 (considered as observed) and 6-hourly wind speed from ERA-20C and daily wind speed from Cordex simulation, respectively, so that the corrected historical distributions of ERA-20C and Cordex match that of ERA-5. The bias is learned on the
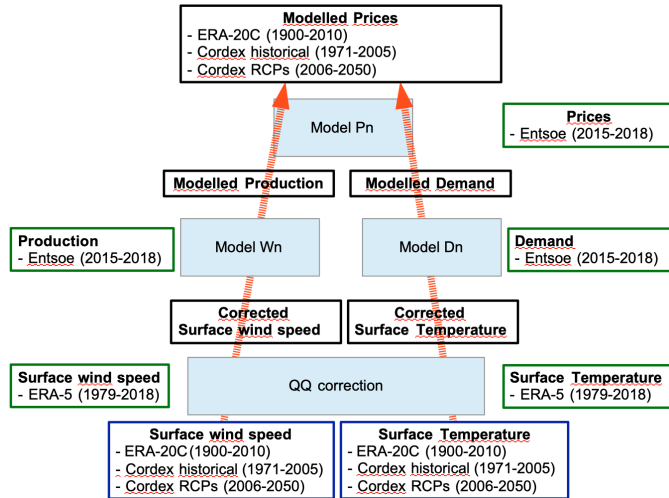

Figure 2: Model scheme for country prices

period common to ERA-5 and ERA-20C, as well as the period common to ERA-5 and historical Cordex simulation. The correction is then applied to the remaining period in ERA-20C and to the RCPs to obtain very long time series. In the second step of the scheme, two models are used to obtain, from corrected wind speed and temperature, the production of wind energy at national level and the electricity demand, respectively.

The parameters of the models are fitted with ENTSOE observed data of wind energy production and electricity production on the period from Jan 1, 2015 to Dec 31, 2018. The models Dn and the model Wn are described in the appendix A and B, respectively. In the third step, a model for day-ahead prices is used to compute prices from wind energy production and electricity demand. The parameters of the model are fitted with ENTSOE observed hourly day-ahead prices on the period from Jan 1, 2015 to Dec 31, 2018. The model Pn is described in the appendix C.

Wind energy infeed scenarios Figure 3 shows the scheme for modeling wind energy infeed at each gridpoint of the domain considered. The scheme is also decomposed into three steps. The first step corresponding to quantile/quantile correction to remove bias is common in the two schemes. In the second step, we interpolate the 6-hour wind speed to obtain a statistically coherent time series at the one-hour resolution. The technique is
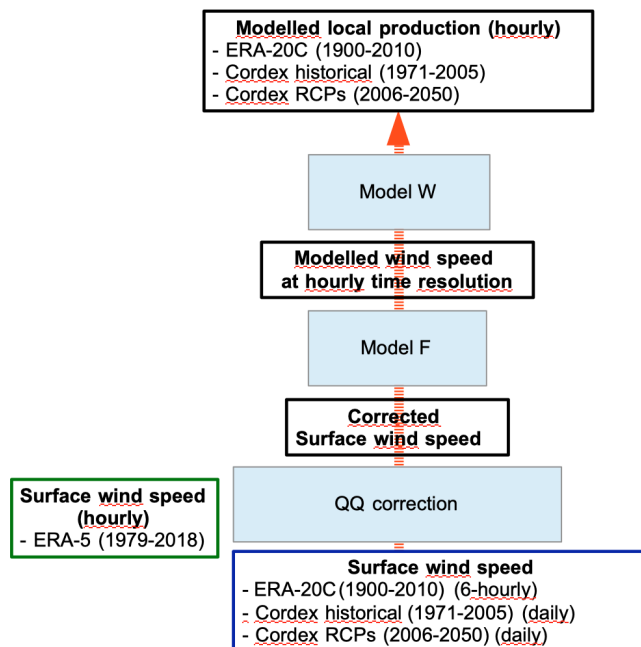

Modelled local production (hourly)
- ERA-20C (1900-2010)
- Cordex historical (1971-2005)
- Cordex RCPs (2006-2050)

Model W

Modelled wind speed at hourly time resolution

Model F

Corrected Surface wind speed

QQ correction

Surface wind speed (hourly)
- ERA-5 (1979-2018)

Surface wind speed
- ERA-20C (1900-2010) (6-hourly)
- Cordex historical (1971-2005) (daily)
- Cordex RCPs (2006-2050) (daily)

Figure 3: Model scheme for local production

based on simulating the missing values from an Ornstein-Uhlenbeck process, conditionned on the observed values, whose parameters are fitted to the hourly wind speed time series from ERA-5. The model F is described in the appendix D. The third step of the scheme consists in extrapolating the wind speed at the hub height using power law with $\alpha = 1/7$ [Justus et al., 1976] and applying a typical power curve adapted for onshore and offshore wind turbines to the modelled hourly wind speed at hub height to obtain the local production (see appendix D).

2.3 Model validation

Figure 4 displays the time series of monthly mean prices observed (ENTSOE) and modelled between January 1, 2015 and Decmber 31, 2017, as well as the distributions of hourly prices for the same period in France (Fig 4-(a,b)), Germany (Fig 4-(c,d)) and Denmark (Fig 4-(e,f)). Time series of monthly prices show a satisfying correlation (0.74)
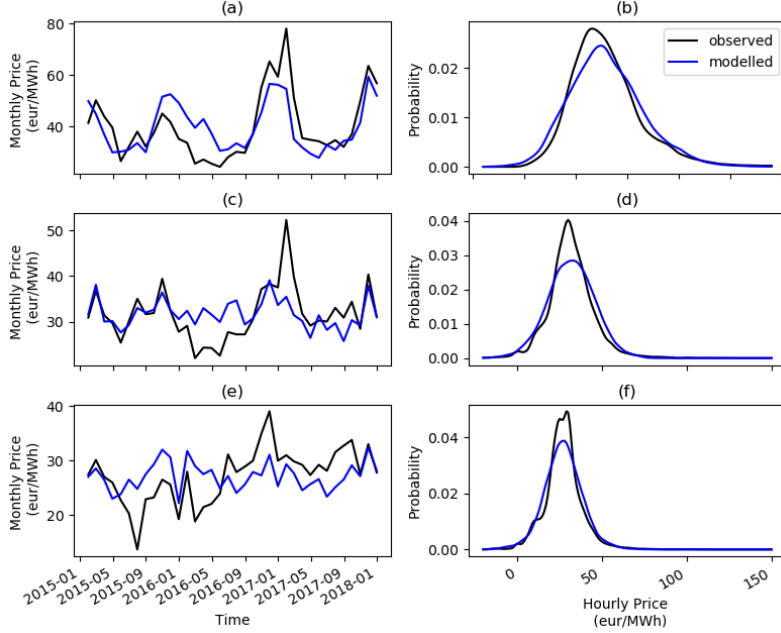

Figure 4: Time series (left) of mean monthly prices and estimated probability density function of hourly prices for the period between January 1st, 2015 and December 31st, 2017. Black curves correspond to observations observed prices and blue ones to model-generated prices. (a, b): France; (c, d): Germany; (e, f): Denmark.

in France due to a well modelled seasonal cycle (Fig 4-(a)). Several peaks and lows are well reproduced by the model, in December 2017 for instance. In Germany, the correlation (0.56) is also satisfying, even if the seasonal cycle seems to be underestimated (Fig 4-(c)). The peaks during winter of 2016/2017 are not well reproduced in France and Germany, because they are related to a particular situation in Western Europe when nuclear plants in France had very low availability and the hydroreservoirs had low levels. Our model cannot reproduce such peaks because availability of nuclear and hydro is not taken into account. This kind of special situations are rare and we leave them out of the scope of the paper. Considering the distributions of hourly prices in France and Germany (Fig 4-(b and d), respectively), we find that the distributions of modelled prices have a slightly higher variance than the distributions of observed prices. This indicates that price volatility is slightly overestimated in our model. This may be due to spikes in observed time series which induce small errors in hyperbolic law parameters estimation (see appendix C) and which we choose not to model for simplicity.

7

In Denmark, the model seems to be less efficient as the correlation between observed and modelled monthly prices is lower (0.31, significant at 0.05 confidence level) (Fig 4-(e)). Indeed, in Denmark, electricity prices are much more volatile and more subject to spikes than in France and Germany which makes them harder to model. Still, the distributions of observed and modelled hourly prices are close to each other (Fig 4-(f)), with the same kind of volatlity issue as in France and Germany.

To validate the local production model, we use regional monthly capacity factor from the RTE website. We were able to find regional monthly data only for France, so that the validation concerns only the French region. Still, since we use the same model and the same type of wind turbines in all countries considered, the analysis is sufficient to validate the model for all these countries. Figure 5 displays the time series of observed
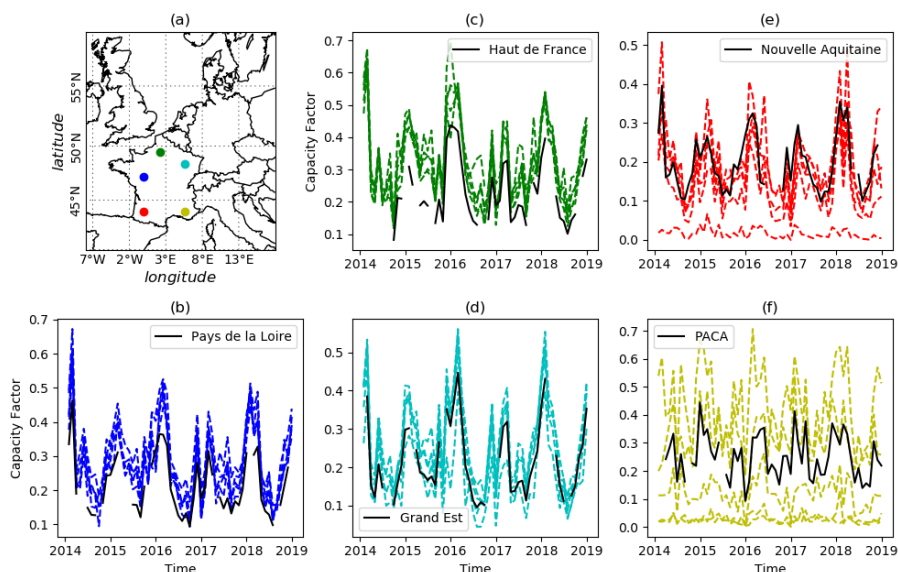

Figure 5: Time series of observed (black) and modelled (dashed colored) monthly capacity factor in five regions of France. (a) map of France displaying local gridpoints used in other panels. (b) Black curve: observed capacity factor in the region 'Pays de la Loire. Dashed blue modelled capacity factor at the gridpoint displayed in panel (a) and four neighboring points, (c,d,e,f) same as (b) for the regions 'Haut de France', 'Grand Est', 'Nouvelle Aquitaine', and 'PACA'.

(black) and modelled (dashed colored) monthly capacity factor in five regions of France (Fig 5-(a)). In the regions 'Haut de France', 'Pays de la Loire' and 'Grand Est' (Fig 5-(b, d, e) respectively), the observed and modelled capacity factors are well correlated, and no large biases are found. In the region 'Nouvelle Aquitaine' (Fig 5-(e)), all but one of the modelled capacity facor time series are close and well correlated to the observed one, and one time series displays a capacity factor close to zero. This is due to the presence Pyrénée mountains south of the gridpoint displayed. Indeed, in moutainous regions reanalysis wind speeds are very low. In the region 'PACA' (Fig 5-(f)), the modelled

capacity factors are broadly distributed between around the observed one. This is typical of this particular region of France which is surrounded by the Alps mountains in the east, the Massif Central (low mountains) in the west and the Mediterranean sea in the south. As a result, the gridpoints located in mountainous regions display low capacity factors, one gridpoint offshore displays a higher capacity factor, and two other points adequately represent the observed capacity factor.

2.4 Wind Farm Revenues and Value

The value of a wind production asset is determined by the cash flow throughout its lifetime. We make the assumption that all of the wind farm production is sold on the day-ahead market.[3] Thus, in our case, the cash-in (or revenues) over a period of length T (say, a year) are calculated as :

$$R_T = \sum_{t=1}^{T} W_t f_t(P_t) \tag{1}$$

with T is the length of the time period considered (in hours), W_t the production at time t in MWh, P_t the day-ahead price at time t in €/MWh, and f_t the function which takes into account the subsidy and payment to the aggregator.

We model both the feed-in-tariff (FiT) and the feed-in-premium (FiP) subsidy. Under FiT, the producer receives a fixed guaranteed price of 82€/MWh for 10 years, after which the price decreases linearly over 5 years to 28€/MWh. After 15 years the subsidy disappears and the remaining energy is sold in the day-ahead market. This corresponds to the support mechanism used in France (until 2016). The function f_t in this case is given by

$$f_t^{FiT} = 82€/\text{MWh}\,\mathbf{1}_{0 \leq t < 10} + \left(82 - 54\frac{(t-10)^+}{5}\right)€/\text{MWh}\,\mathbf{1}_{10 \leq t < 15} + P_t\mathbf{1}_{t>15}.$$

Under FiP, the producer receives a guarateed bonus of 33€/MWh in addition to the market price if the resulting amount is less than 78€/MWh and only the market price otherwise. After 15 years the subsidy disappears and the remaining energy is sold in the day-ahead market. This corresponds to the support mechanism used in Denmark. The function f_t is in this case given by

$$f_t^{FiP} = (P_t + 33€/\text{MWh})\mathbf{1}_{P_t < 45€/\text{MWh}} + P_t\mathbf{1}_{P_t \geq 45€/\text{MWh}}.$$

Germany used a FiT mechanism similar to the French one until 2012 and now uses a FiP similar to the Danish one. We use the same mechanisms for onshore and offshore wind farms.

The cash-out can be divided into two categories : the capital expenditures (CAPEX) which correspond essentially to the initial investment, and the operational expenditures

---

[3]In practice, the individual renewable energy producers are usually paid by the aggregator at the day-ahead market prices reduced by a small constant aggregator fee.

Costs	Onshore	Offshore	Source
Capex	1350 k€/MW	3000 k€/MW	Turbine, grid connection
Fixed Opex	20 k€/MW/yr	60 k€/MW/yr	O&M, balancing costs

Table 3: Costs of onshore and offshore wind farms

(OPEX). Recent literature shows a decrease of investment costs for onshore and offshore wind turbines in Europe, which range from 1.2M€/MW to 2.0M€/MW for onshore wind turbines ([Lantz et al., 2012], [RC. Thomson, 2015], [Ioannis et al., 2017]) and from 3.0M€/MW to 4.4M€/MW for offshore turbines ([RC. Thomson, 2015, Ioannis et al., 2017, Bosch et al., 2019]). In [RC. Thomson, 2015], the annual fixed OPEX are suggested to be 1.5% and 2.0% of the CAPEX for onshore and offshore wind turbines respectively. The costs used in our study are summarized in table 3 and are inspired by [RC. Thomson, 2015].

The value of a wind farm is quantified by the net present value (NPV) indicator, which is written as follows.

$$NPV = \sum_{t=1}^{T}(C_t^{in} - C_t^{out})(1 + r)^{-t} \qquad (2)$$

where T is the duration of the project in years, C_t^{in} stands for the revenues of the wind farm in year t, and C_t^{out} represents the costs of the wind farm during the year t :

$$C_t^{out} = Capex_t + Opex_t. \qquad (3)$$

The CAPEX will of course only be invested at time $t = 0$. The parameter r is known as the discount rate, it reflects the time value of money and the intrinsic risk of the project. The value of r used in the study is 0.05, and corresponds to the low range of values found in the literature (see [Ioannis et al., 2017] for instance). The net present value is very senstive to the discount rate, which is an important source of uncertainty in the quantification of wind farm value.

3 Variability of revenues and uncertainty of the wind farm value using past century data

In this section we analyze the variability of wind farm revenues and the associated value uncertainty based on past climate data. Using our models presented in Section 2.2 with ERA20C reanalysis as meteorological inputs, we simulate very long fictitious trajectories of national electricity prices, national electricity consumption and national wind production for France, Germany and Denmark, and use parts of these long time series as possible future scenarios over which the variability of wind farm revenues is analyzed. The analysis thus focuses on natural climate variability, but anthropogenic climate change is not taken into account, with the exception of a small trend in temperature values which appears already in the 20th century.

3.1 Variability of production and prices

Figure 6 displays the relative standard deviation (RSD) of the onshore and offshore production (capacity factor) (Fig 6-(a)) and of the price in each country (Fig 6-(b)). The RSD is the ratio between the standard deviation and the mean. Comparing RSD values in Figure 6-(a,b), we conclude that the variability of revenues is dominated by the variability of the capacity factor. The standard deviation of the price is around 35% of
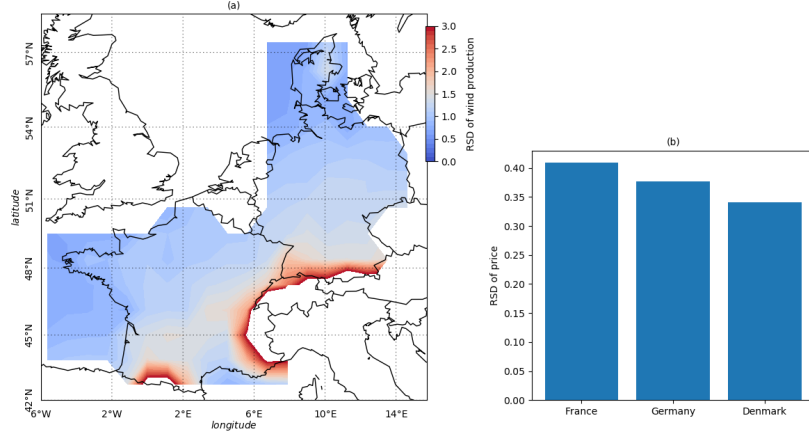

Figure 6: Relative Standard Deviation (RSD) of the capacity factor onshore (green) and offshore (blue) (a) and of the prices (b) in the 3 countries considered. The RSD is the ratio of the standard deviation and the mean.

the mean price while it exceeds the mean for the capacity factor, in most onshore regions, especially in locations where the mean is low (e.g mountainous regions). In France, the RSD of the price exceeds 45% (Fig 6-(b)), because the seasonal cycle is more pronounced than in the other countries, due to strong seasonal variations of the consumption.

Figure 7 displays the trends (10 years sliding mean) of electricity prices, eletricity consumption and wind energy production in France, Germany and Denmark (Fig 7-(a,b,c), respectively). It shows that prices are highly correlated with consumption as expected. Prices and wind energy production exhibit very low correlation, although one could expect them to be negatively correlated, because higher wind production increases energy supply. Long term trends are identified in consumption and prices, especially after the late 60s when they both decrease. Very long-term trends in wind energy production are found. Wind energy production increases in all three countries from the beginning until late 20th century and appears to decrease afterwards. [Wohland et al., 2019] identify such positive trends for wind speed in ERA20C, CERA20C reanalyses as well as in the OFA observation dataset (assimilated in these reanalyses). They also identify negative trends in NOAA20CR reanalysis, and no trends in the free simulation ERA20CM which uses the same model as ERA20C. The study focuses on North-Pacific and North Atlantic areas, but smaller but significant trends are found in continental Europe as well. They show that the positive trends in ERA20C may come from the assimilation of marine wind speed. The discussion of the reality of these trends is very instructive but still
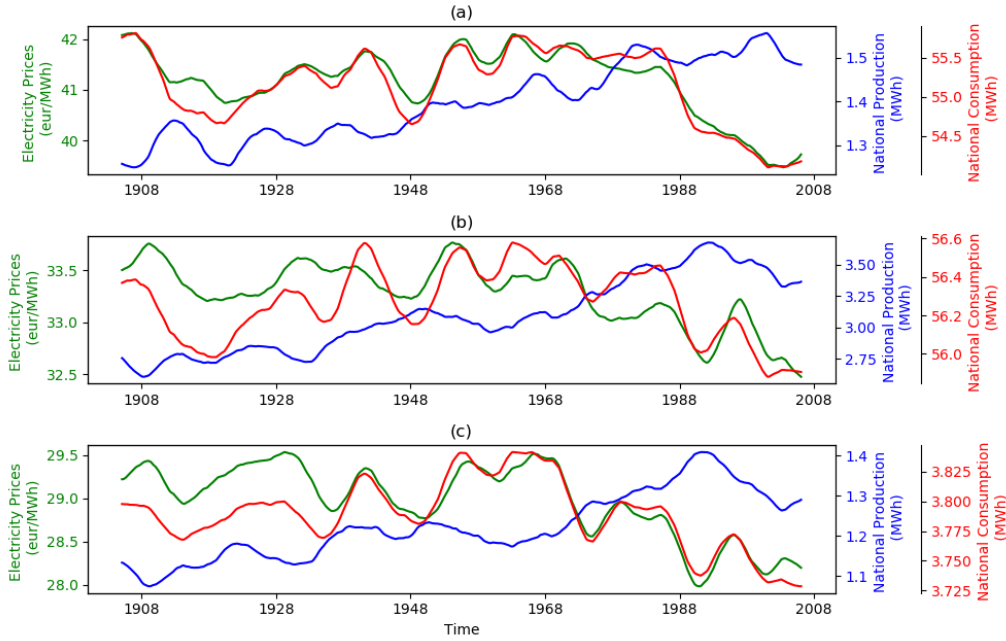
Figure 7: Trends of prices (green lines), national electricity consumption (red lines) and national wind energy production (blue lines) in (a) France, (b) Germany, (c) Denmark.

does not clearly conclude on the fact that these trends are spurious or not. Arguments in favor of spurious trends are based on the changes in wind measurement techniques, the disagreement between mean sea level pressure (MSLP) over the Arctic in ERA20C and measurements (HadSLP2), and the low signal on wind speed in CMIP5/CORDEX simulations. Nevertheless, there are also some arguments in favor of real trends such as the findings of trends in wave height in agreement with positive wind speed trends. We make the choice to keep the wind speed as it is in ERA20C. This choice can be justified by, firstly, the purpose of a reanalysis which aims at representing the observations in the best possible way, and secondly, the fact that there is no proper correction methodology. In the following, we adress this issue by giving in some cases an order of magnitude of the impact of this trend on our results.

Figure 8 shows the correlation between prices and production at different timescales. At the hourly timescale (Fig 8-(a)), the correlation between prices and production is low but positive (<0.2). At the monthly timescale (Fig 8-(b)), the wind energy production is highly positively correlated with prices in all three countries under study. This indicates a strong correspondance in seasonal cycles of wind energy production and prices. Indeed, prices are high during cold seasons when demand increases. At the same time, the production is also expected to be high in Western Europe due to the enhanced activity of the storm track during fall and winter. In the long term (Fig 8-(c)), the correlation between wind energy production and prices becomes negative, especially in the Northern region. This may be related to the merit-order effect : wind production increase at
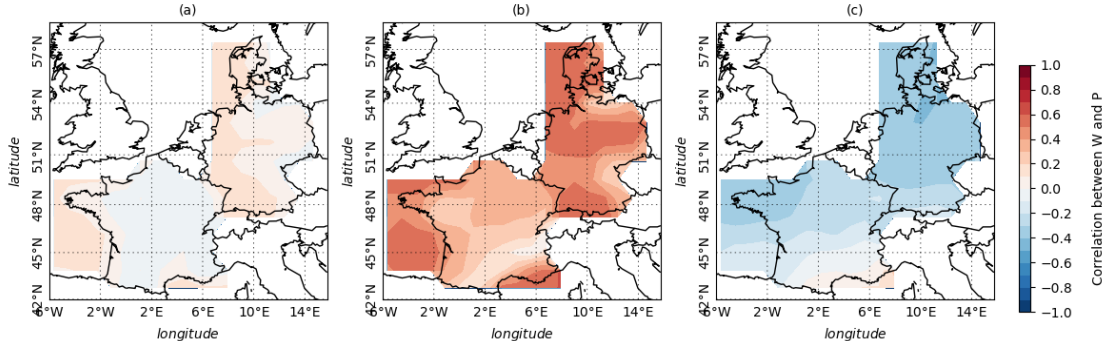
12

Figure 8: Pearson correlation between prices and production (a) hourly mean, (b) monthly mean, (c) yearly mean

the national level tends to decrease prices (see [Cludius et al., 2014, Clò et al., 2015] for instance). It also may indicate a correlation between temperature (whose increase tends to decrease demand, thus prices) and wind energy production. This correlation can also be related to the large scale weather regimes such as the North Atlantic Oscillation (NAO) which, in the positive phase, enhances the storm track activity, increasing the wind production in Western Europe, an at the same time brings warmer wet air in this region thus decreasing energy demand and prices. In the negative phase, this phenomenon is reversed. The NAO displays long term cycles of the order of 3 to 7 years. Many studies have shown the relation of the NAO (and other weather regimes) with wind speed and production and electricity demand (see for instance [Boccard, 2009, Grams et al., 2017]).

3.2 Monthly variability of revenues

Figure 9 displays the Value at Risk at 95% level (VaR_{95}) of the monthly revenues and of the net monthly revenues (cash flow). The VaR_{95} is defined as the 5th percentile, so that it shows the lowest revenue (resp. net revenue) level which the farm is sure to earn 95% of the time.

To compute the wind farm revenues, three situations are considered : (i) wind farms selling all production in the day-ahead market (Fig 9-(a,b)) with no subsidy; (ii) wind farms supported with FiT mechanism of 86eur/MWh (Fig 9-(c,d)); and (iii) wind farms supported with FiP mechanism (Fig 9-(e,f)). In the absence of subsidies, the VaR_{95} of revenues and net revenues range from less than 1000 to 8000 eur/month/MW and from -4000 to 5000 eur/month/MW, respectively. The VaR_{95} of revenues is larger offshore than onshore due to higher capacity factor (Fig 9-(a)). The VaR_{95} of net revenues does not change much between offshore and onshore areas, due to higher costs for offshore wind farms (Fig 9-(b)). Net revenues are positive in North Western areas, as well as in the Southeast of France. For a wind farm supported by FiT mechanism, VaR_{95} of revenues and net revenues ranges from less than 1000 to 21000 eur/month/MW and

13

from -2000 to 19000 eur/month/MW, respectively. Maximum values of both revenues and net revenues are obtained for offshore wind farms. For a wind farm supported by FiP mechanism, VaR_{95} of revenues and net revenues ranges from less than 1000 to 15000 eur/month/MW and from -3000 to 13000 eur/month/MW, respectively. For FIT and FiP support mechanism, VaR_{95} of net revenues is positive almost everywhere, except in mountainous regions (e.g the Alps).
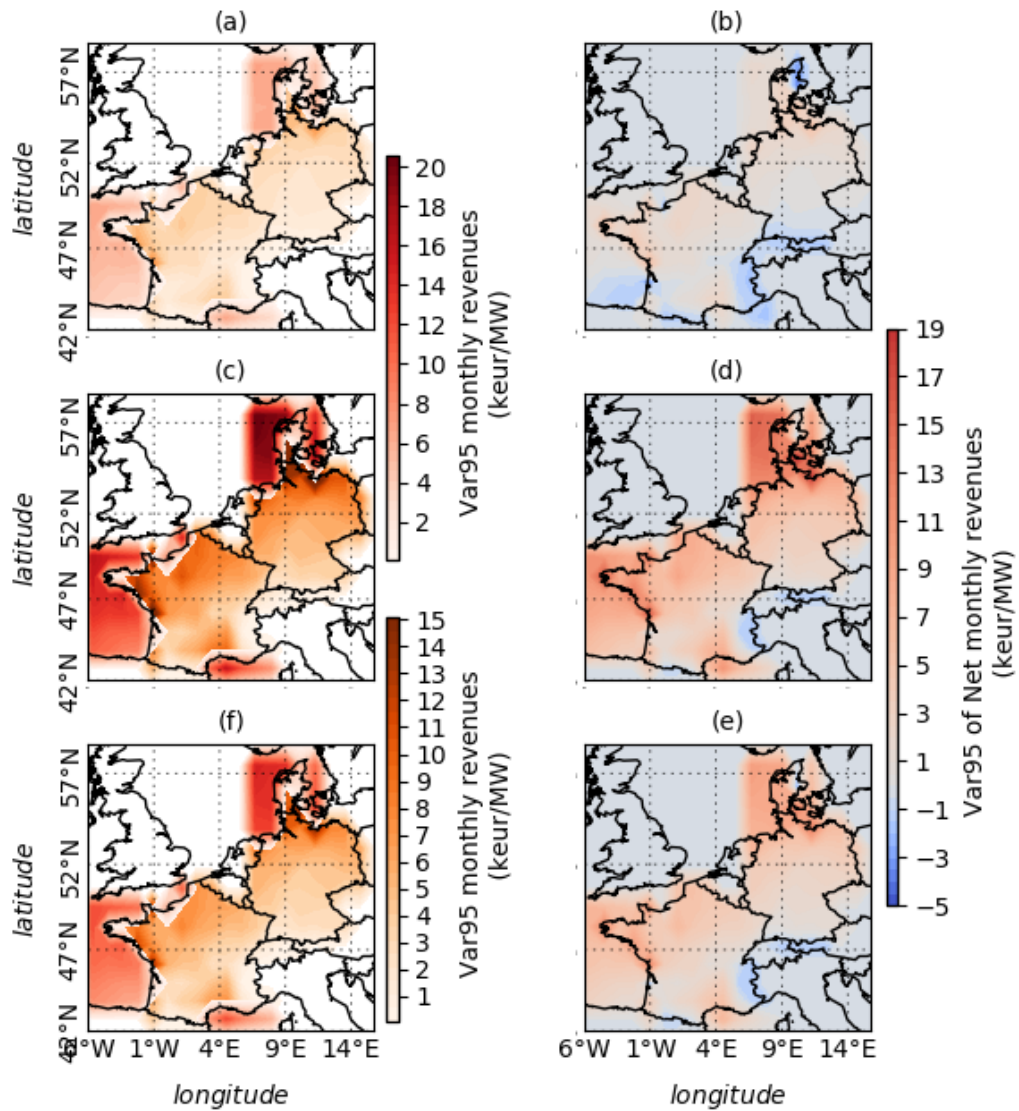

Figure 9: 95*th* Value at Risk of monthly revenues (left) and net monthly revenues (right), (a,b) for production sold on the spot market, (c,d) for production sold with a FiT support mechanism of 86eur/MWh, and (e,f) for production sold with a FiP support mechanism.

3.3 Year to year variability of revenues

Figure 10 displays the mean (left panels) and the standard deviation (right panels) of the yearly revenues for wind farms selling all the production in the day-ahead market (Fig 9-(a,b)), wind farms supported with FiT mechanism of 86eur/MWh (Fig 9-(c,d)), and wind farms supported with FiP mechanism (Fig 9-(e,f)). In all three situations, the standard deviation of the revenues varies from 5 to 27% of the yearly revenues, which indicates that price variations have low impact on the variability of revenues at the yearly timescale since FiT corresponds to constant prices. For wind farms operating without subsidy (Fig 9-(a,b)), the standard deviation and the mean of revenues are higher in France than in Germany and Denmark, mainly due to higher prices. In France, the mean price is around 41 euros, in Germany, 36 euros, and in Denmark, 31 euros. In this case, the mean annual revenues reach at most 210keur/MW/yr. For wind farms supported by FiT mechanism (Fig 9-(c,d)), the mean revenues may be higher than 400keur/MW/yr onshore and offshore. For wind farms supported by FiP mechanism (Fig 9-(e,f)), the mean revenues may be over 300keur/MW/yr onshore and offshore. In Germany, mean revenues display a North/South gradient with high revenues in the north and low revenues in the south. The standard deviation of revenues follows the same pattern. In Denmark, highest revenues are found offshore. In France, highest onshore revenues are found in the northwestern coastal region. In the southeast, high mean revenues are found in the region where the Mistral blows. The Mistral region is also associated with high variability of the revenues.

Removing the trends in ERA20C wind speed to model local production results in an increase of mean yearly revenues of the order of 2 to 3% and a decrease of the standard deviation of the order of 2 to 3% onshore, except in the southeast of France, where the decrease is of 10 to 12%. Offshore, the standard deviation decrease is of the order of 10% (close to shore) to 15% (further from coast).

3.4 Value of a wind farm over its lifetime

We now extend the period of interest to the lifetime of a wind farm in order to quantify the variability of its value. To do so, we define 81 virtual wind farm projects at each grid-point starting on the 1st of January of each year from 1900 to 1981 and lasting 30 years. Figure 11 displays the mean NPV (Fig 11-(a)) after 30 years as well as the corresponding VaR_{95} (Fig 11-(b)) computed from the 81 virtual wind farm projects defined in this way. For offshore wind farms, the NPV is negative almost everywhere due to the high initial investment. Thus, offshore wind farms are not yet profitable if not supported by regulations mechanisms. Nevertheless, both investment costs and operational costs are decreasing rapidly ([Junginger and Turkenburg, 2004, Sovacool et al., 2017, Williams et al., 2017]). For onshore wind farms, a virtual line can be drawn from southwest of France to northeast of Germany defining an area northwest where wind farms are profitable, and southeast where they are not. An exception is found in the southeast of France where strong regional winds blow all year round. Comparing the mean NPV (Fig 11-(a)) with the VaR_{95} of the NPV (Fig 11-(b)), we notice very small differences, meaning that the NPV
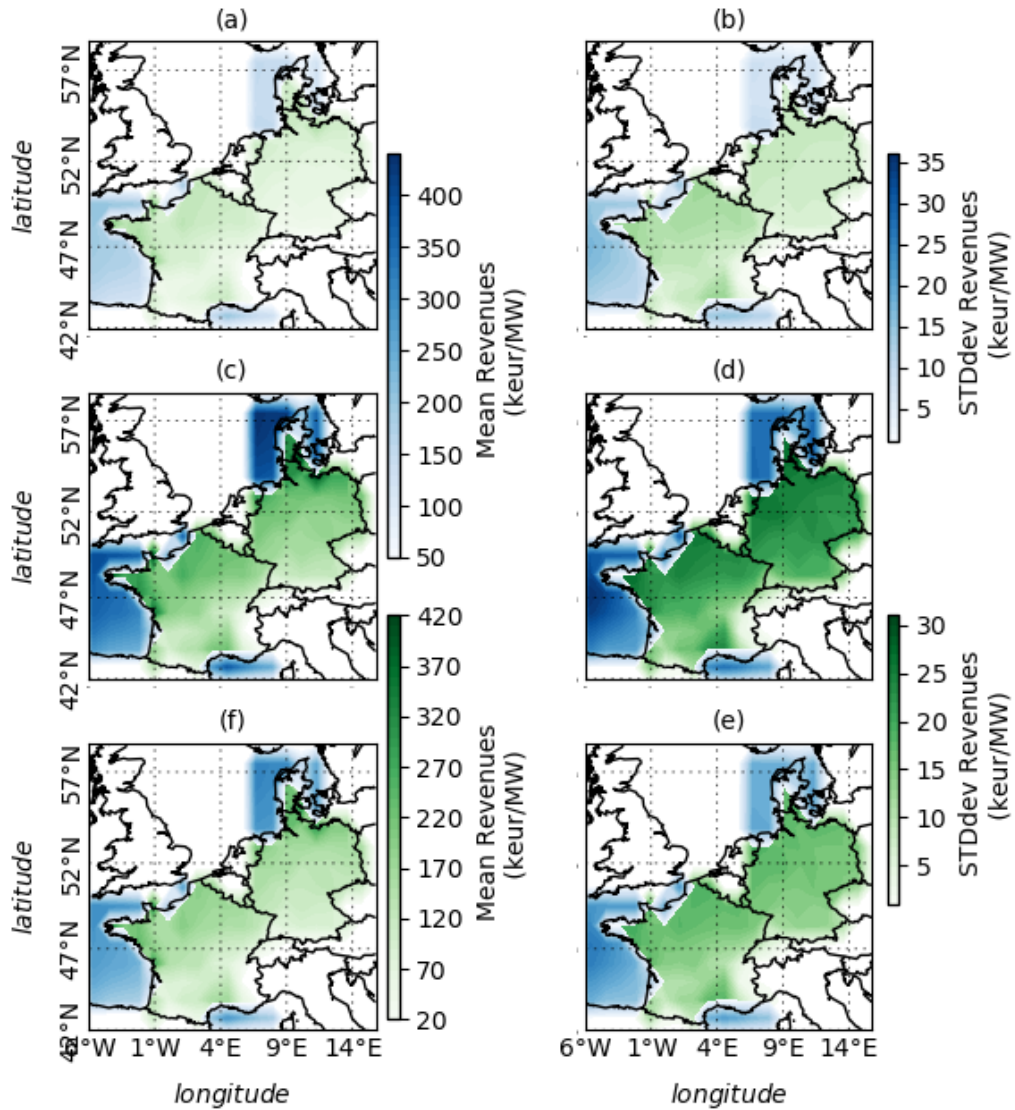
Figure 10: Mean (left) and standard deviation (right) of yearly revenues for onshore (green) and offshore (blue) wind farms. The mean and standard deviation are calculated over the period of ERA20C spanning from 1900 and 2010. (a,b) for production sold on the spot market, (c,d) for production sold with a FiT support mechanism of 86eur/MWh, and (e,f) for production sold with a FiP support mechanism.

does not vary much on the long term. Note that removing the trends in the ERA20C wind speed to compute local production has a large impact on the inter-quartile range (IQR) (difference between the 75th and the 25th percentile of NPV over the 81 projects), as using detrended production results in an IQR which is 30% to 100% less than the IQR using production with trends. In other words, the very long term trends in wind

speed result in low profitability early in the century and higher profitability at the end of the century. Detrending wind speed results in a less varying profitability along the $20^{t}h$ century.The decrease in IQR is larger for offshore wind farms, and onshore wind farms close to coast.
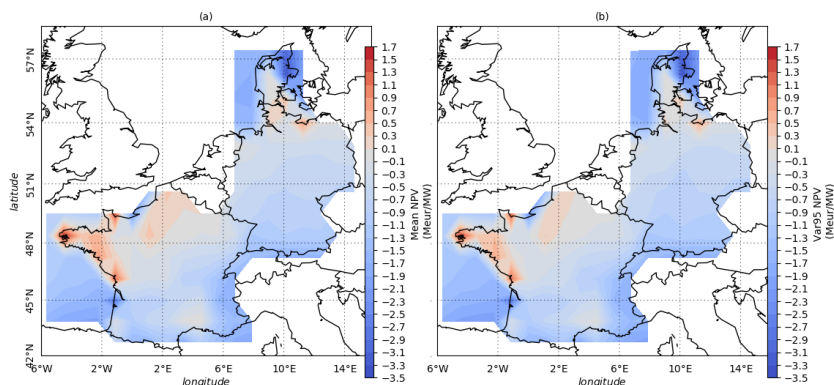

Figure 11: Net present value after 30 years of lifetime for wind farms operating without a subsidy (a) mean over the 81 wind farm projects (b) Value at risk 95th over the 81 wind farm projects

Figure 12 displays the same quantities as Figure 11, but for wind farms supported by FiT (Fig 12-(a,b))and FiP (Fig 12-(c,d)). It shows that support mechanisms increase the wind farm value, especially the FiT mechanism. In particular, offshore wind farms are found to be profitable with FIT in the Western coast of France, Denmark and Germany. The mean NPV over the 81 projects for the FIT mechanism reaches 3.0M€/MW for a wind farm with a lifetime of 30 years (Fig 12-(a)). For FIP mechanism, the mean NPV reaches 2.5M€/MW.

3.5   Sensitivity of NPV to the discount rate

The discount rate is a parameter which strongly impacts the NPV, and as a a consequence the profitability of an asset. Throughout the paper, we use a discount rate of $r = 0.05$. In order to quantify the impact of the discount rate on our results we compute mean NPV over the 81 projects defined above in 6 locations and for values of r from 0.0 to 0.1 with increment 0.01. The results of this sensitivity analysis are displayed in Figure 13. In the case of wind farms operating without a subsidy (Fig 13-(b)), wind farms at the 6 locations considered show a negative mean NPV for $r > 0.06$. With $r = 0.05$, only wind farms located in France display a positive mean NPV. With a null discount rate, these three wind farms show a NPV of about $1.5Meur/MW$. In the case of wind farms supported by FiT mechanism (Fig 13-(c)), whatever the discount rate value, the mean NPV stays positive for onshore wind farms considered. From $r = 0.0$ to $r = 0.1$, the loss in mean NPV ranges from $1.5Meur/MW$ (red curve) to $2.7Meur/MW$ (blue curve). For the offshore location considered (in yellow), the sensitivity of NPV to the discount
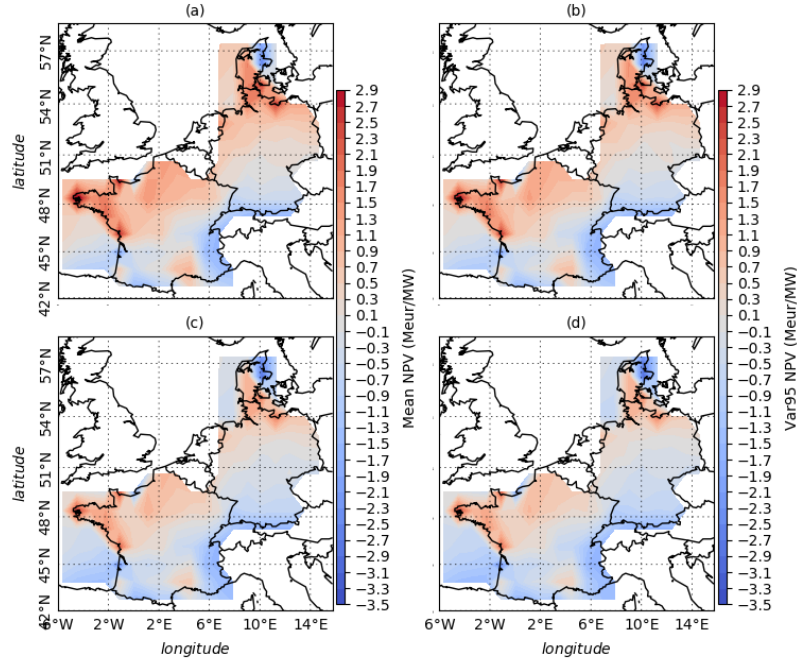
Figure 12: Net present value of wind farms supported by FIT (a, b) and FIP (c,d) mechanisms after 30 years of lifetime (a,c) mean over the 81 wind farm projects (b,d) Value at risk 95th over the 81 wind farm projects

rate is much higher, because of the higher costs. The mean NPV becomes negative for discount rate values in excess of 0.07. In the case of wind farms supported by FiP mechanism (Fig 13-(d)), the NPV sensitivity to the discount rate is comparable to that of FiT mechanism, but the NPV values are lower.

3.6 Historical based projection uncertainty on futur value of wind farms

For a wind farm project, it is common to base the projections of the future value of an asset on the historical wind speed recorded at the location considered. To analyze the error resulting from such approach, we now define 51 wind farm projects at each gridpoint starting on the firs of January of each year from 1930 to 1981 and lasting 30 years. We use three different strategies for estimating the wind farm value : one based the wind speed recorded during 5 most recent years, one based on the 10 most recent years, and the last one based on 30 most recent years before the project begins.

Figure 14 displays the mean and 90th percentile of the absolute error (out of 51 virtual projects : from 1930 to 1981) between projected cumulative revenues based on recent past years and actual revenues. We compare projections based on a historical period of 5-years (Fig 14-(a,d)), 10-years (Fig 14-(b,e)), and 30-years (Fig 14-(c,f)).

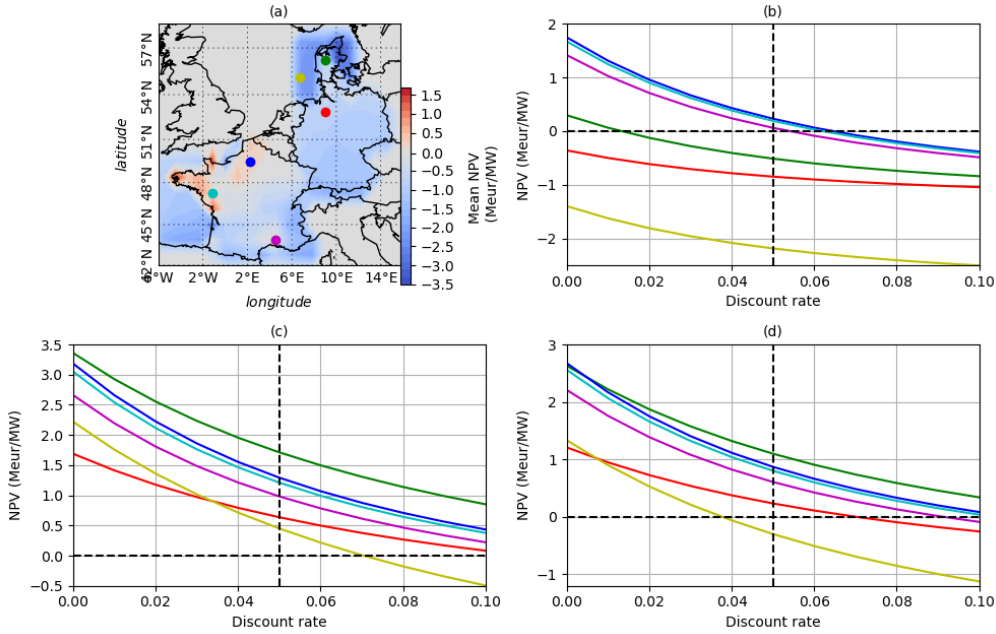Using the past 30-years to project future revenues results in a larger mean absolute

18

Figure 13: (a) Map of the mean NPV value for wind farms not supported by mechanism, with $r = 0.05$ (same as Fig 11-(a)), the gridpoints scattered correspond to the curves in the sensitivity plots (b,c,d). (b) Mean NPV in case of no support mechanism as a function of the discount rate for the 6 locations ploted in (a) ; (c) and (d) same as (b) but for wind farms supported by FIT and FIP mechanisms respectively.

error than using 5 or 10 past years (Fig 14-(a) compared to (b) and (c)). Nevertheless, the 90th percentile of the absolute error over the 51 projects is larger when using the 5 past years of data than when using the past 10 or even 30 years (Fig 14-(d) compared to (e) and (f)). Thus, using the past 5 years results in higher risk to make large errors than when the projection is based on a longer period (e.g 10 or 30 years). Using 30 years of data makes the projection more sensitive to very long term trends, resulting in a larger mean error, while using less historical years makes the projection more sensitive to shorter term interannual variability of revenues. Such projections can sometimes largely overestimate or underestimates actual future production, revenues, and wind farm value. For instance, if an investor projects future revenues based on the past 5 years when the NAO is in positive phase, he may highly overestimate future production concluding wrongly on the profitability of the project.

Note that this result is very sensitive to long term trends found in ERA-20C wind speed (see section 3.1). Indeed, the fact that the mean error is larger for a 30 years based projection than a 5 years based projection, is entirely due to these trends. When trends are removed from the data, using the past 30-years to project future revenues results in a lower mean absolute error than when using 5 or 10 past years, so that this method is considered as the best in terms of both mean and extreme errors.
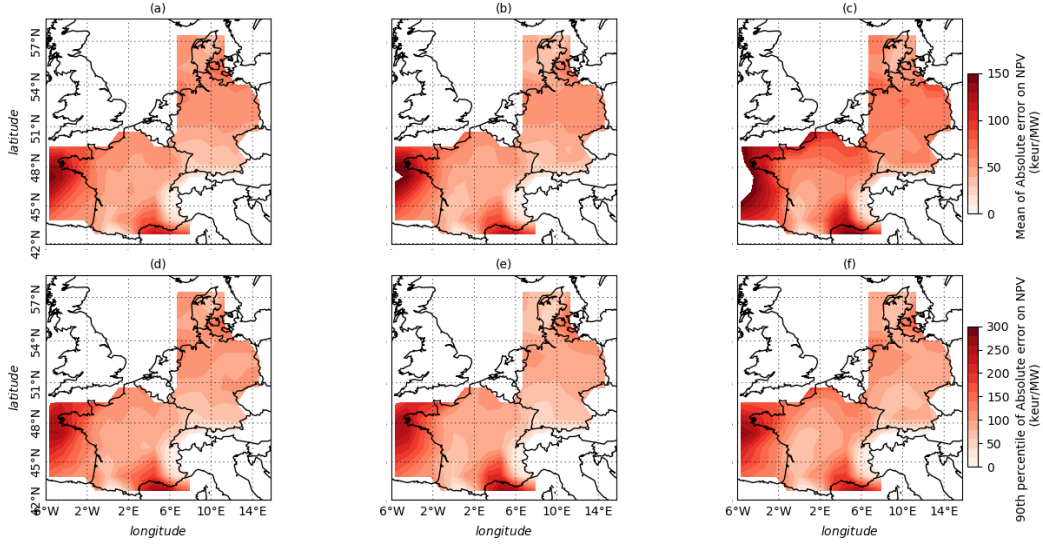
Figure 14: Average (a,b,c) and 90th percentile (d,e,f) of the absolute error calculated between the NPV at the end of a project and the projected NPV based on (a,d) the past 5 years (b,e) the past 10 years (c,f) the past 30 years

4 Scenarios for future

4.1 Future prices scenarios

Prices scenarios are created by making an assumption on the future trends of electricity demand in Europe as well as on future penetration of wind energy in each country. The surface temperature and surface wind speed from the CORDEX dataset are used as inputs of demand and national wind production models. Three scenarios for the electricity demand are created. In the first scenario, the electricity demand is only temperature dependent. As a result of temperature increase in the RCPs scenarios, the electricity demand tends to decrease in this scenario. In the second and the thrid scenarios, we project a medium and high electrification, respectively. The trends of electricity demand are based on the IMAGE 3.0 scenarios LIMITS-Pledges and LIMITS-baseline ([Stehfest et al., 2014]). In the scenario of medium and high electrification, the electricity demand trends correspond to an increase of 28% and 42% of initial mean demand from 2020 to 2050, respectively. The trends are defined relatively to each country historical demand, but the increase follows a common trend defined for Europe. We use two different scenarios for wind energy penetration in each country considered. They are based on [WindEurope, 2017] scenarios for 2030. The projected installed capacities in each scenario and country are given in the table 4 which summarizes the different scenarios for prices.

Prices are thus projected using these scenarios for electricity demand, wind energy production in each country as well as using the temperature and wind speed from the

RCP-45 and RCP-85			Electricity Demand		
			No trends	Medium	High
Wind energy penetration	Low	France	/ 31.0 GW onshore 4.3 GW offshore	28 % demand increase 31.0 GW onshore 4.3 GW offshore	42 % demand increase 41.0 GW onshore 11.1 GW offshore
		Germany	/ 60.0 GW onshore 14.0 GW offshore	28 % demand increase 60.0 GW onshore 14.0 GW offshore	42 % demand increase 60.0 GW onshore 14.0 GW offshore
		Denmark	/ 3.6 GW onshore 3.4 GW offshore	28 % demand increase 3.6 GW onshore 3.4 GW offshore	42 % demand increase 3.6 GW onshore 3.4 GW offshore
	High	France	/ 41.0 GW onshore 11.1 GW offshore	28 % demand increase 41.0 GW onshore 11.1 GW offshore	42 % demand increase 41.0 GW onshore 11.1 GW offshore
		Germany	/ 71.0 GW onshore 20.0 GW offshore	28 % demand increase 71.0 GW onshore 20.0 GW offshore	42 % demand increase 71.0 GW onshore 20.0 GW offshore
		Denmark	/ 6.5 GW onshore 6.1 GW offshore	28 % demand increase 6.5 GW onshore 6.1 GW offshore	42 % demand increase 6.5 GW onshore 6.1 GW offshore

Table 4: Wind energy penetration and electricity demand scenarios used to build prices scenario in each country

two RCPs as inputs. We thus obtain in each country, for each CORDEX run, and for each model, 60 different price projections (2 RCPs, 5 models, 3 demand scenarios and 2 penetration scenarios). In the following, the two RCPs are considered as two simulations, not as scenarios, because the results from one RCP to the other are not significantly different. This is not unexpected as RCP scenarios begin to show diverging trajectories around 2050 in terms of global mean temperature for instance. Projecting prices with our models after 2050 also shows diverging trajectories at this period (Not shown).

Figure 15 displays the projected yearly mean prices in the 6 scenarios described previously, and in each country considered. The filled areas are defined by the maximum and minimum price among the 5 simulations and 2 RCPs. Some discontinuities are visible in 2020 (Fig 15- (c), (d), (e) and (f)). They correspond to the start of demand electrification and wind energy penetration scenarios. Price trajectories span a wide range of possible prices (from less than about 20€/MWh in 2050 in Denmark (Fig 15-(b)) to 70€/MWh in 2050 in France (Fig 15-(e))). The 10 simulations (filled area) do not display uncertainties of the order of magnitude of 3€/MWh. The trajectories of the scenarios are first driven by electricity consumption assumptions (comparing panels from top to bottom), second by wind energy penetration assumptions (comparing left and right panels), and third by the RCP followed (Not shown).

In the scenario where the demand only depends on temperature, the prices drop slowly between 2010 and 2050 (Fig 15-(a,b)). For a medium and high electrification of
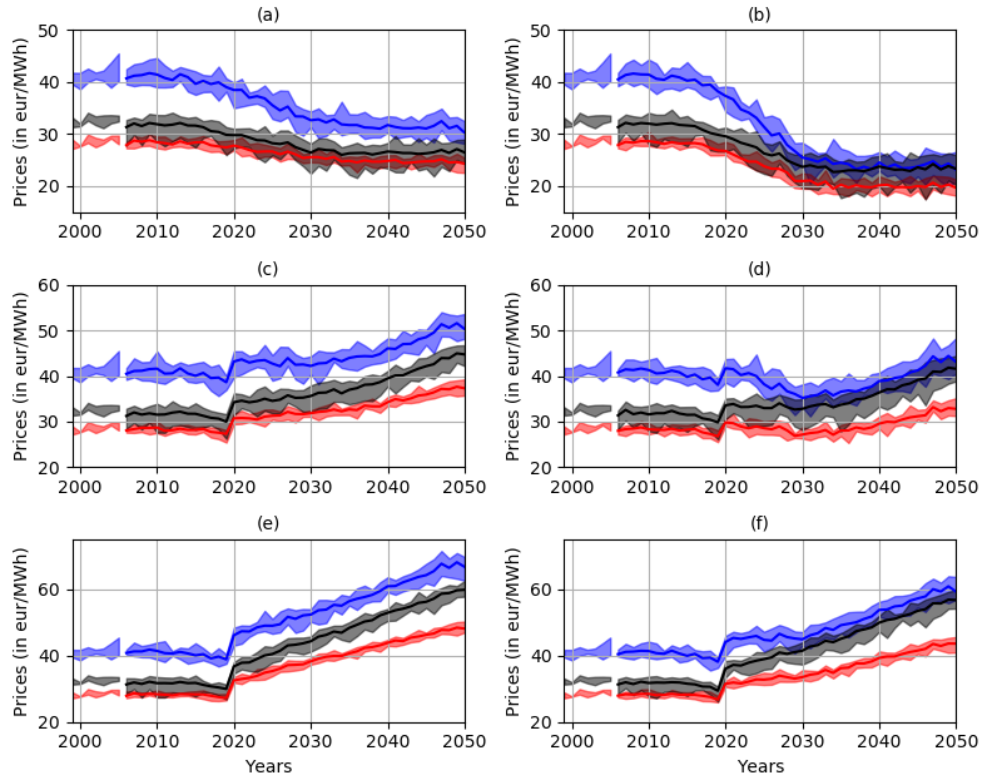
Figure 15: Yearly mean price projections in each country, in blue for France, in black for Germany, in red for Denmark, for each of the 6 different scenarios. The shaded area corresponds to the minimum and maximum yearly mean prices among the 10 simulations (5 models and 2 RCPs). Left panels correspond to low penetration scenarios (a,c,e) and right panels to high penetration scenarios(b,d,f). Top panels correspond to no demand trend scenarios (a,b), middle panels to medium demand trend scenarios (c,d), and bottom panels to high demand trend scenarios (e,f).

the system, the electricity demand increases after 2020, and proportionnally so do the prices (Fig 15-(c,d,e,f)).

Figure 16 shows the projected intra-annual RSD of prices for each scenario. The scenario of low demand and high penetration displays high values of RSD in all countries (Figure 16-(b)). The increasing standard deviation relatively to the average price is due to decreasing mean prices, but also to increasing standard deviation due to the intermittency of wind energy production. Overall, there is an increase of the price RSD in every scenario due to wind energy penetration.

Overall, there is an increase of the price RSD in every scenarios with high wind energy penetration. The increase in RSD takes place between 2020 and 2030 when the installed wind capacity increases. In France, there is a decrease of the RSD after 2030
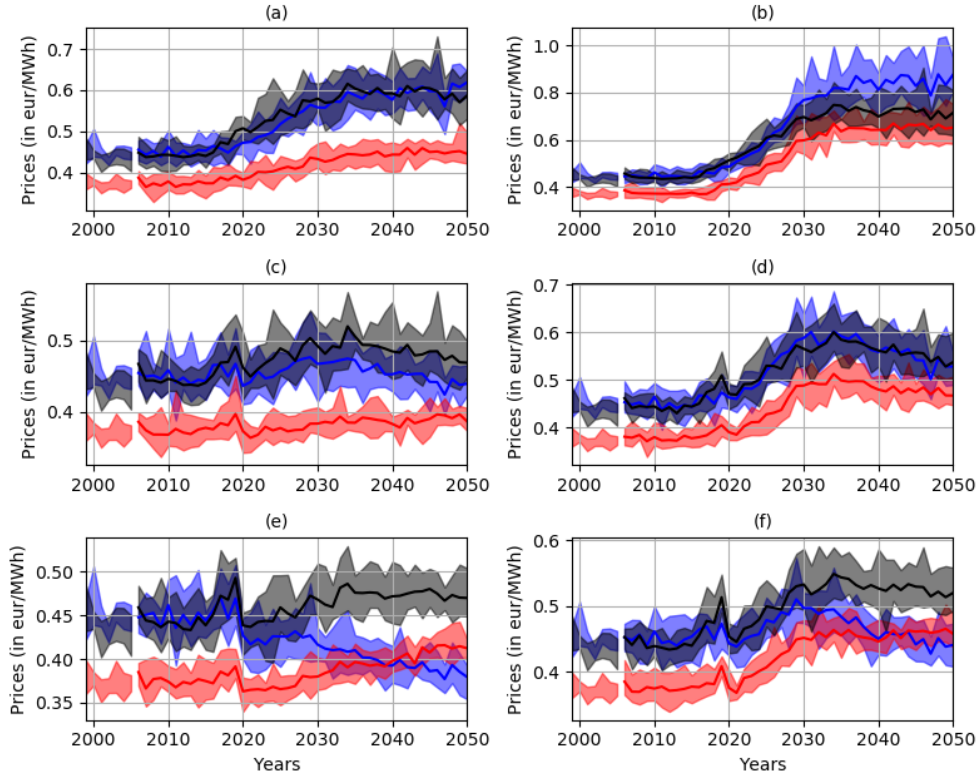
Figure 16: Same as Figure 15 but for relative standard deviation

in the scenarios of medium and high electrification of demand and high penetration of wind energy (Fig 16-(d) and (f)), and a decrease of RSD after 2020 in the scenario of high electrification of demand and low penetration (Fig 16-(e)). We conclude that the penetration of renewable have less influence on prices variability in France than in Denmark and Germany.

4.2   Future local production projections

The change in future wind speed and future wind production has already been investigated in several studies. Tobin et al. (2016) using the same CORDEX dataset (with 12 models) found a decrease of the wind speed by the end of the century of less than 2% and a decrease of the wind power generation potential in Western Europe of about 5 to 10%. We obtain similar results with our dataset (Not shown).

4.3   Value of wind farms under future climate scenarios

The NPV is projected in the future for virtual wind farms commissioned on the 1st of January 2021 with lifetime of 30 years (decommissioning date is the 31st of December

23

2050). Figure 17 displays the averaged NPV over the 10 CORDEX simulations (5 models and 2 RCPs) at the end of the wind farm lifetime in 2050, for each of the 6 price scenarios, in the case of wind farms which do not claim for support mechanism. As expected, the worst scenario for wind farms profitability is the scenario with no electrification of demand and a high penetration of wind energy (Fig 17-(a)). Indeed, due temperature increase, the electricity demand decreases as well as prices. Moreover, the high penetration of wind energy has for effect to decrease spot prices. The scenario with no electrification of demand and a low penetration of wind energy (Fig 17-(b)) is also not in favor for the same reasons. In these scenarios, under our assumptions, the profitability of wind farms is very low. The average NPV does not exceed 1.5 M€/MW, and is often negative. In the scenarios projecting a high electrification of the demand (Fig 17-(c,d)), the NPV is positive almost over the entire onshore domain. the mean NPV reach values over 3.0M€/MW in these scenarios. For offshore wind farms, low positive NPV are found in the northwest of France in the scenario of high electrification and low penetration ((Fig 17-(d)). In the scenarios projecting a medium electrification of the demand (Fig 17-(e,f)), the differences due to wind energy penetration is exacerbated compared to no electrification or high electrification scenarios. Indeed, in medium electrification scenarios, the NPV of wind farms is often positive in the low penetration scenario (Fig 17-(f)) and negative in the high penetration scenario (Fig 17-(e)). The highest NPV in these scenarios reaches 2.4M€/MW.
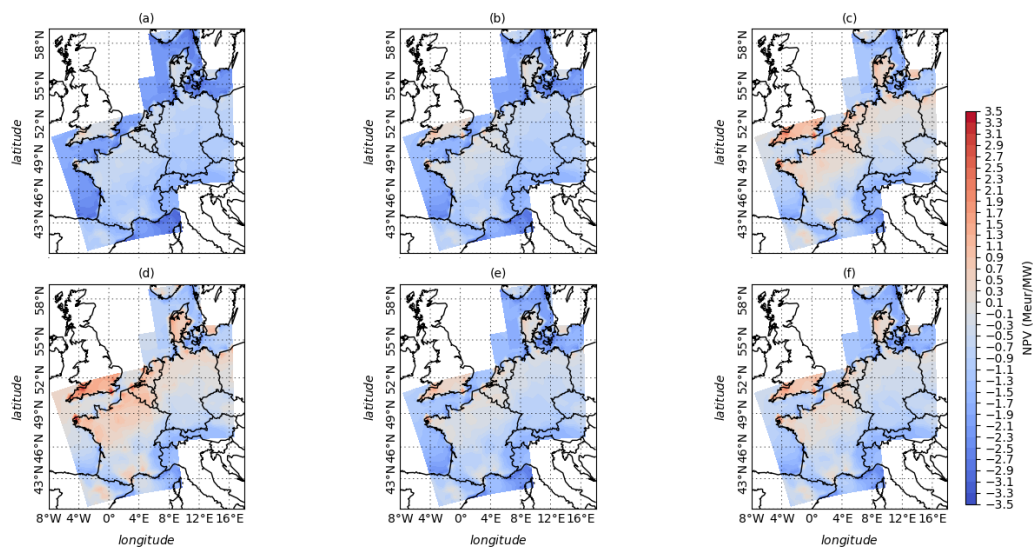

Figure 17: Net present value, averaged over the 10 CORDEX simulations (5 models and 2 RCPs), for the 6 prices scenarios. (a) No demand trends and high wind penetration , (b) No demand trends and low wind penetration,(c) High demand trends and high wind penetration, (d) High demand trends and low wind penetration, (e) Medium demand trends and high wind penetration, (f) Medium demand trends and low wind penetration.

24

Figure 18 displays the averaged NPV over the 10 CORDEX simulations (5 models and 2 RCPs) at the end of the wind farm lifetime in 2050, for each of the 6 price scenarios, in the case of wind farms supported by a FiT mechanism. In every scenarios, onshore wind farms in the northwest of France, north of Germany, and Denmark are profitable. Offshore wind farms in the northwest of France and western Denmark are found profitable even in the worst scenario (i.e no electrification of demand and high penetration of wind energy (Fig 18-(a))). In the scenarios of high electrification (Fig 18-(c) and (d)), the mean NPV can be more than 4.5M€/MW in several locations close to coast, and the NPV is positive almost on the entire domain.
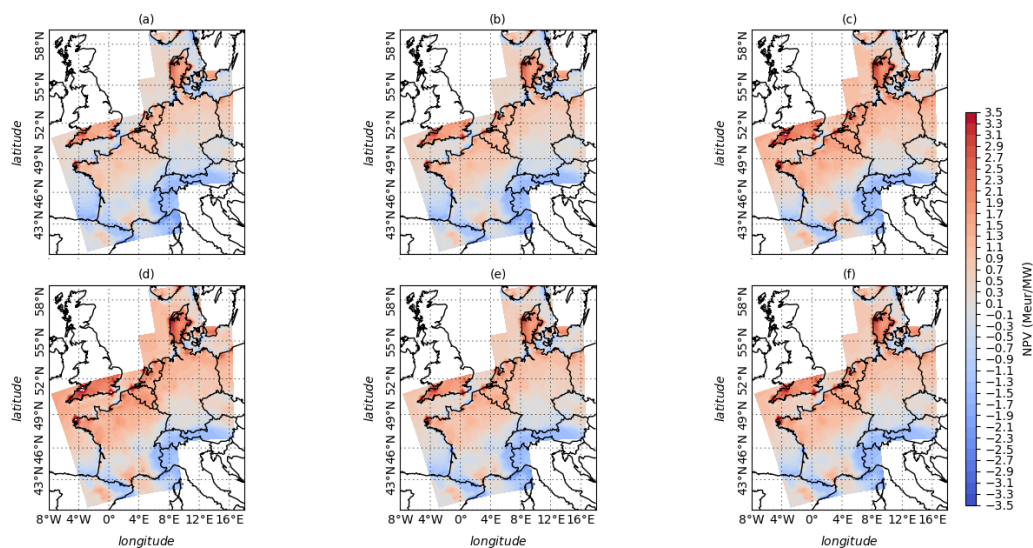

Figure 18: Same as Figure 17, but for wind farms supported with a feed-in-tariff mechanism.

Figure 19 displays the averaged NPV over the 10 CORDEX simulations (5 models and 2 RCPs) at the end of the wind farm lifetime in 2050, for each of the 6 price scenarios, in the case of wind farms supported by a FiP mechanism. In the scenarios of high electrification (Fig 19-(c) and (d)), the mean NPV is positive almost on the entire domain as well. The NPV can reach more than 4.0M€/MW in several locations close to coast. Offshore wind farms are also found profitable in these scenarios. This is not the case for scenarios of no and medium electrification.

5 Conclusion

In this paper, we studied the variability of wind farm revenues and value in past and future climate, in France, Germany and Denmark. The study using past climate data evaluates the impact of climate variability where the study using future climate projections evaluates the impact of climate change and future electrification and renewable
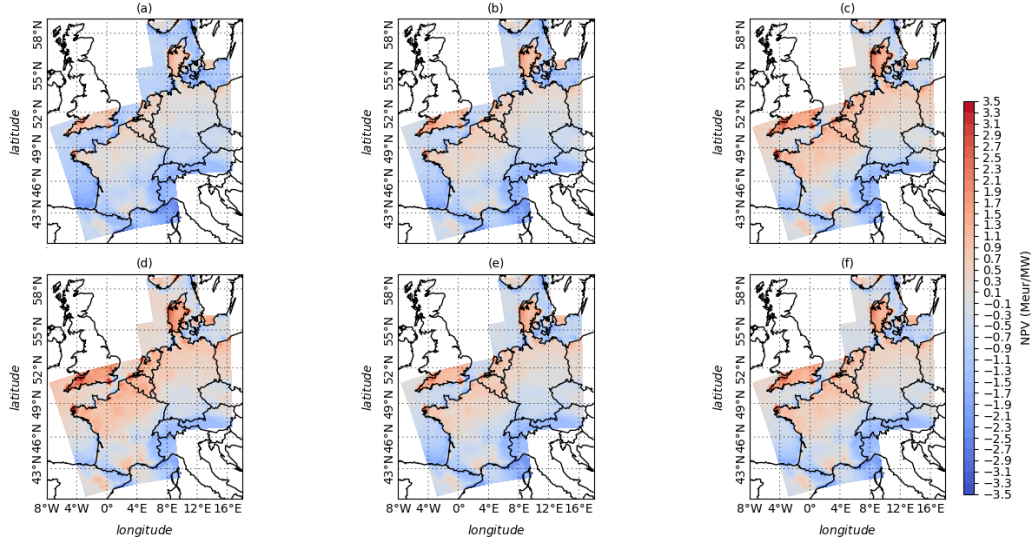
Figure 19: Same as Figure 17, but for wind farms supported with a feed-in-premium mechanism.

penetration scenarios. Based on past climate scenarios, we quantify the mean and the 95%-quantile of the net present value of a reference wind power plant located in different areas of the three countries under study. We find that, in the absence of subsidies, the NPV is positive in 95% of the scenarios only in some areas in the West and North of France and in the North opf Germany / South of Denmark. On the other hand, in the presence of feed-in premium subsidy, most onshore zones, with the exception of mountaneous regions, become profitable, and under feed-in tariffs, the profits are even higher and become positive even for some offshore zones. Under future climate, the profitability of wind power plants depends on the subsidy level, but also on the scenarios for electricity demand and wind energy penetration.

6   Acknowledgement

Appendices

A   Demand Model (Model Dn)

The daily electricity demand is modelled as a function f of the mean daily surface temperature T_t in France at time t, and of threshold temperatures T_h with h for "hot"

and T_c with c for "cold":

$$D_t^n = f^w(T_t, T_h, T_c)\mathbf{1}_{t \in W} + f^o(T_t, T_h, T_c)\mathbf{1}_{t \in O} + \epsilon_t \tag{4}$$

Here, T_h and T_c are parameters, which are found by nonlinear least squares, W is the set of weekdays, O is the set of weekend days/holidays, and ϵ_t is a residual.

The functional forms are specified as follows,

$$f^{wo}(T_t, T_h, T_c) = a_0^{wo} - a_h^{wo}(T_t - T_h)^+ + a_c^{wo}(T_c - T_t)^+. \tag{5}$$

B National Production Model (Model Wn)

The daily wind energy production is computed from observed data from ENTSOE. The daily wind speed at 10m is first extrapolated to 100m (hub height) using the power law with $\alpha = 1/7$ (Justus et al. (1976)):

$$F_{100} = F_{10} \times \left(\frac{100}{10}\right)^\alpha \tag{6}$$
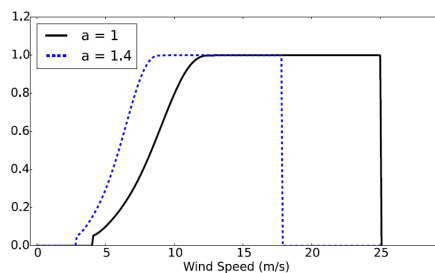

Figure 20: Power curve of a Vestas-90-2MW Turbine with normalized power

Next, the power curve of Figure 20 is applied at each gridpoint with $a = 1.0$. We compute the mean wind energy production W_n^0 onshore and offshore as :

$$W_{n,t}^0 = \frac{\sum_{i=1}^N W_{t,i}}{N} \times C_t^{inst}$$

with $W_{t,i}$ the power computed at each gridpoint and C_t^{inst} the installed capacity in the given country at time t. A bias still exists between computed and observed production because the installed capacity is observed at the country scale. In order to correct this bias, we apply, separately for onshore and offshore production, a linear least square regression to obtain W_n. Adapting the a parameter to obtain more realistic capacity factors (Fig 20) for each offshore and onshore location would lead to comparable results. However, we prefer to correct the bias using the observed national production data from ENTSOE.

C Day-ahead Price Model (Model P)

Let us denote the hourly price as $P_{j,h}$ and the daily price as P_j, and let $\Delta(P_{j,h}) = P_{j,h} - P_j$. We denote weekdays and weekend days/holidays with superscripts ^{w} and ^{o}, respectively, as for the demand model, and the superscript ^{wo} means that the expression holds both for weekdays and for weekends.

We first decompose $\Delta(P_{j,h}^w)$ and $\Delta(P_{j,h}^o)$ using Principal Component Analysis as :

$$\Delta(P_{j,h}^w) = \overline{E_h^w} + \sum_{p=1}^{N} E_{p,h}^w Z_{p,j}^w + \epsilon$$

$$\Delta(P_{j,h}^o) = \overline{E_h^o} + \sum_{p=1}^{N} E_{p,h}^o Z_{p,j}^o + \epsilon$$

Here $\overline{E_h}$ is the mean daily cycle around P_j, $E_{p,h}$ is the pth mode of variation of the daily cycle and $Z_{p,j}$ is the so called principal component that shows how the given mode of variation evolves with time.

In our price model, we fix the number of principal components to $N = 3$ and model the dynamics of X_j and $Z_{1,j}, \ldots, Z_{N,j}$. Introduce the vectors

$$X_j^w = \begin{pmatrix} P_j^w \\ Z_{1,j}^w \\ \vdots \\ Z_{N,j}^w \end{pmatrix} \qquad \text{and} \qquad X_j^o = \begin{pmatrix} P_j^o \\ Z_{1,j}^o \\ \vdots \\ Z_{N,j}^o \end{pmatrix}$$

The dynamics of each vector is described by an autoregressive model involving the demand D_j, the national wind production W_j, seasonal and autoregressive components.

$$X_j^{wo} = a^{wo} D_j + b^{wo} D_j^2 + \sum_{i=1}^{L=3} l_i^{wo} D_{j-i} + c^{wo} W_j$$
$$+ \alpha_{sin}^{wo} \sin(\frac{2\pi j}{365}) + \alpha_{cos}^{wo} \cos(\frac{2\pi j}{365}) + \beta^{wo} X^{wo}{}_{j-1} + \epsilon_j^{wo}.$$

The parameters a^{wo}, b^{wo}, l_i^{wo}, α_{sin}^{wo}, α_{cos}^{wo}, β^{wo} are fitted by least square regression. We assume that the residuals ϵ_j follow a hyperbolic distribution, whose parameters are estimated by maximum likelihood.

The full model for the price process can then be written :

$$P_{j,h} = \mathbf{1}_{j \in W} \left(P_j^w + \sum_{p=1}^{N} E_{p,h}^w Z_{p,j}^w \right) + \mathbf{1}_{j \in O} \left(P_j^o + \sum_{p=1}^{N} E_{p,h}^o Z_{p,j}^o \right),$$

where, as before, W denotes the set of weekdays and O is the set of weekend days/holidays.

D Local wind speed and production Models (Model F & W)

The model F aims at generating an hourly wind speed time series from the 6-hourly (resp. daily) wind speed from ERA-20C reanalysis (Cordex simulations) that is statistically consistent with hourly wind speed from ERA-5 reanalysis.

Assume that the logarithm of the wind time series, $X_t = \log(V_t)$, is an Ornstein-Uhlenbeck process with dynamics :

$$dX_t = k(\theta - X_t)dt + \sigma dW_t$$

The explicit form of the OU process is

$$X_s = X_0 e^{-ks} + \theta(1 - e^{-ks}) + \sigma \int_0^s e^{-k(s-r)}dW_r$$

The stationnary law of this process is

$$N\left(\theta, \frac{\sigma^2}{2k}\right),$$

and the autocorrelation in the stationary regime is $\rho(s,t) = e^{-k(t-s)}$. The model parameters σ, k and θ can thus be easily estimated from the mean, variance, and autocorrelation of the log-wind time series.

We would like to characterize the law of X_s given X_t for $0 < s < t$. It is clear that the conditional law of X_s given X_t is Gaussian. We thus only need to characterize the mean $\mathbb{E}[X_s|X_t]$ and the variance $Var[X_s|X_t]$.

Let
$$\alpha = \frac{Cov(X_s, X_t)}{Var[X_s|X_t]} = e^{-k(t-s)}\frac{1 - e^{-2ks}}{1 - e^{-2kt}}$$

Then, X_t is independent from $X_s - \alpha X_t$. Therefore,

$$\mathbb{E}[X_s|X_t] = \mathbb{E}[X_s - \alpha X_t + \alpha X_t|X_t] = \alpha X_t + \mathbb{E}[X_s - \alpha X_t]$$
$$= \alpha X_t + X_0 e^{-ks} + \theta(1 - e^{-ks}) - \alpha(X_0 e^{-kt} + \theta(1 - e^{-kt}))$$

and

$$Var[X_s|X_t] = Var[X_s - \alpha X_t + \alpha X_t|X_t] = Var[X_s - \alpha X_t]$$
$$= \sigma^2 \frac{1 - 2e^{-2ks}}{2k}\left(1 - \alpha e^{-k(t-s)}\right) \tag{7}$$

With these known values of mean and variance, on can easily simulate the value of X_s. This enables us to simulate the 10m wind speed at the hourly time resolution, which we denote in the following by F_{10m}, by interpolating the 6-hour time series.

The model W aims at modelling the local wind energy production from F_{10m}. We first extrapolate wind speed to $100m$ height using power law [Justus et al., 1976]:

$$F_{100m} = F_{10m} \times \left(\frac{100}{10m} \right)^{\alpha} \tag{8}$$

with $\alpha = \frac{1}{7}$.

Finally, we apply the power curve of a Vestas-90 (2MW) wind turbine (Fig 20) with normalized power to obtain the local wind capacity factor. In order to take into account differences between onshore and offshore wind turbines, we define $a_{onshore}$ and $a_{offshore}$ to be equal to 1.28 and 0.82, respectively. The values of $a_{onshore}$ and $a_{offshore}$ have been chosen to obtain an average capacity factor onshore and offshore of 25% and 35%, respectively.

References

[Boccard, 2009] Boccard, N. (2009). Capacity factor of wind power realized values vs. estimates. *Energy Policy*, 37:2679–2688.

[Bosch et al., 2019] Bosch, J., Staffell, I., and Hawkes, A. (2019). Global levelised cost of electricity from offshore wind. *Energy*, 189.

[Clò et al., 2015] Clò, S., Cataldi, A., and Zoppoli, P. (2015). The merit order effect in the italian power market : The impact of solar and wind generation on national wholesale electricity prices. *Energy Policy*, 77:79–88.

[Cludius et al., 2014] Cludius, J., Hermann, H., Matthes, F., and Graichen, V. (2014). The merit order effect of wind and photovoltaic electricity generation in germany 2008?2016: Estimation and distributional implications. *Energy economics*, 44:302–313.

[Damm et al., 2017] Damm, A., Koberl, J., Prettenthaler, F., Rogler, N., and Toglhofer, C. (2017). Impacts of 2c global warming on electricity demand in europe. *Climate Services*, 7:12–30.

[Gatzert and Kosub, 2016] Gatzert, N. and Kosub, T. (2016). Risks and risk management of renewable energy projects: The case of onshore and offshore wind parks. *Renewable and Sustainable Energy Reviews*, 60:982–998.

[Gatzert and Vogl, 2016] Gatzert, N. and Vogl, N. (2016). Evaluating investments in renewable energy under policy risks. *Energy Policy*, 95:238–252.

[Giorgi et al., 2008] Giorgi, F., Jones, C., and Asrar, G. (2008). Addressing climate information needs at the regional level: The cordex framework. *WMO Bull*, 53.

[Grams et al., 2017] Grams, C., Beerli, R., Pfenninger, S., Staffel, I., and Wernli, H. (2017). Balancing europe s wind power output through spatial deployment informed by weather regimes. *Nature climate change*, 7:557–564.

[Hersbach and Dee, 2016] Hersbach, H. and Dee, D. (2016). Era5 reanalysis is in production. *ECMWF Newsletter*, 147.

[Hitzeroth and Megerle, 2013] Hitzeroth, M. and Megerle, A. (2013). Renewable energy projects: Acceptance risks and their management. *Renewable and Sustainable Energy Reviews*, 27:576–584.

[I4CE, 2019] I4CE (2019). Towards an alternative approach in finance to climate risks:taking uncertainties fully into account.

[Ioannis et al., 2017] Ioannis, K., Ioannis, T., and Nikolaos, K. (2017). Investment evaluation in renewable projects under uncertainty, using real options analysis: The case of wind power industry. *Investment Management and Financial Innovations*, 14:96–103.

[Junginger and Turkenburg, 2004] Junginger, H. and Turkenburg, W. (2004). Cost reduction prospects for offshore wind farms. *Wind Engineering*, 28.

[Justus et al., 1976] Justus, C., Hargreaves, W., and Yalcin, A. (1976). Nationwide assessment of potential output from wind powered generators. *Journal of Applied Meteorology*, 15:673–678.

[Lantz et al., 2012] Lantz, E., Wiser, R., Hand, M., Arapogianni, A., Cena, A., Simonot, E., and JamesSmith, E. (2012). Iea wind task 26 : The past and future cost of wind energy.

[Poli et al., 2016] Poli, P., Hersbach, H., Dee, P., Berrisford, P., Simmons, J., Vitart, F., Laloyaux, P., Tan, D. G. H., Peubey, C., Thépaut, J., Trémolet, Y., Hólm, E., Bonavita, M., Isaksen, L., and Fisher, M. (2016). Era-20c: An atmospheric reanalysis of the twentieth century. *Journal of Climate*, 29(11):4083–4097.

[Pryor and Barthelmie, 2010] Pryor, S. and Barthelmie, R. (2010). Climate change impacts on wind energy: A review. *Renewable and Sustainable Energy Reviews*, 14:430–437.

[Pryor et al., 2006] Pryor, S., Barthelmie, R., and Schoof, J. (2006). Inter-annual variability of wind indices across europe. *Wind Energy*, 9:27–39.

[Pryor et al., 2005] Pryor, S. C., Schoof, J. T., and Barthelmie, R. J. (2005). "empirical downscaling of wind speed probability distributions". *Journal of Geophysical Research*, 110:D19109.

[RC. Thomson, 2015] RC. Thomson, G. H. (2015). Life cycle costs and carbon emissions of wind power. *University of Edinburgh*.

[Sovacool et al., 2017] Sovacool, B. K., Enevoldsen, P., Koch, C., and Barthelmie, R. J. (2017). Cost performance and risk in the construction of offshore and onshore wind farms. *Wind Energy*, 20(5):891–908.

[Stehfest et al., 2014] Stehfest, E., Vuuren, D., Kram, T., Bouwman, A., Alkemade, R., Bakkenes, M., Biemans, H., Bouwman, A., Elzen, M., Janse, J., Lucas, P., van Minnen, J., Muller, M., and Prins, A. (2014). *Integrated Assessment of Global Environmental Change with IMAGE 3.0. Model description and policy applications*.

[Tobin et al., 2016] Tobin, I., Jerez, S., Vautard, R., Thais, F., van Meijgaard, E., Prein, A., Déqué, M., Kotlarski, S., Maule, C. F., Nikulin, G., Noel, T., and Teichmann, C. (2016). Climate change impacts on the power generation potential of a european mid-century wind farms scenario. *Environ. Res. Lett.*, 11.

[Tobin et al., 2015] Tobin, I., Vautard, R., Balog, I., Bréon, F., Jerez, S., Ruti, P., Thais, F., Vrac, M., and Yiou, P. (2015). Assessing climate change impacts on european wind energy from ensembles high-resolution climate projections. *Climatic Change*, 128:99–112.

[Wenz et al., 2017] Wenz, L., Levermann, A., and Auffhammer, M. (2017). North–south polarization of european electricity consumption under future warming. *Proceedings of the National Academy of Sciences*.

[Williams et al., 2017] Williams, E., Hittinger, E., Carvalho, R., and Williams, R. (2017). Wind power costs expected to decrease due to technological progress. *Energy Policy*, 106.

[WindEurope, 2017] WindEurope (2017). Wind energy in europe : Scenarios for 2030.

[WindEurope, 2019] WindEurope (2019). Financing and investment trends : The european wind industry in 2018.

[Wohland et al., 2019] Wohland, J., Omrani, N., Witthaut, D., and Keenlyside, N. S. (2019). Inconsistent wind speed trends in current twentieth century reanalyses. *Journal of Geophysical Research: Atmospheres*, 124(4):1931–1940.